Available online at www.sciencedirect.com
ScienceDirect
Physics Letters B 643 (2006) 257–262
PHYSICS LETTERS B
www.elsevier.com/locate/physletb

g factors of ^{31,32,33}Al: Indication for intruder configurations in the ^{33}Al ground state

P. Himpe [a], G. Neyens [a,*], D.L. Balabanski [b,1], G. Bélier [c], D. Borremans [a], J.M. Daugas [c], F. de Oliveira Santos [d], M. De Rydt [a], K. Flanagan [a], G. Georgiev [d,2], M. Kowalska [e], S. Mallion [a], I. Matea [d,3], P. Morel [c], Yu.E. Penionzhkevich [f], N.A. Smirnova [g], C. Stodel [d], K. Turzó [a], N. Vermeulen [a], D. Yordanov [a]

[a] *Instituut voor Kern- en Stralingsfysica, K.U. Leuven, Celestijnenlaan 200 D, B-3001 Leuven, Belgium*
[b] *Dipartimento di Fisica, Università di Camerino, I-62032, Camerino, Italy*
[c] *CEA/DIF/DPTA/PN, BP 12, F-91680 Bruyeres le Chatel, France*
[d] *GANIL, BP 55027, F-14076 Caen cedex 5, France*
[e] *Institut für Physik, Universität Mainz, D-55099 Mainz, Germany*
[f] *Joint Institute for Nuclear Research, FLNR, Dubna 141980, Moscow Region, Russia*
[g] *Vakgroep Subatomaire en Stralingsfysica, Universiteit Gent, Proeftuinstraat 86, B-9000 Gent, Belgium*

Received 24 May 2006; received in revised form 10 August 2006; accepted 20 October 2006

Available online 30 October 2006

Editor: V. Metag

Abstract

The g factors of ^{31,32,33}Al have been measured using the β-nuclear magnetic resonance (β-NMR) technique on spin-polarized beams produced in the fragmentation of a ^{36}S (77.5 MeV/u) beam on a ^{9}Be target. Nearly pure beams of Al ($Z = 13$) isotopes were selected with the high-resolution fragment separator LISE at GANIL. An asymmetry as high as 6% has been observed in the β-NMR curve for ^{32}Al implanted in a Si single crystal. The magnetic moment of the $N = 20$ nucleus ^{33}Al is obtained for the first time: $\mu(^{33}\text{Al},\ I^{\pi} = 5/2^{+}) = 4.088(5)\mu_N$, while those of ^{31,32}Al are obtained with improved accuracy: $\mu(^{31}\text{Al},\ I^{\pi} = 5/2^{+}) = 3.830(5)\mu_N$ and $\mu(^{32}\text{Al},\ I^{\pi} = 1^{+}) = 1.9516(22)\mu_N$. Comparison of the results to shell-model calculations in the sd and the sdpf shell-model spaces leads to the conclusion that ^{33}Al must contain some contribution from 2p–2h intruder configurations in its ground-state wave function. This indicates a gradual transition from the normal sd shell Si ($Z = 14$) isotopes to the intruder Mg ($Z = 12$) isotopes.

The gyromagnetic factor (g factor) is a very sensitive probe to the wave function of a nuclear state. Systematic precise measurements of g factors in a chain of isotopes/isotones allow to probe small changes in the nuclear structure with changing isospin. Nuclei near the β-stability line with protons and neutrons filling the sd shell-model orbits ($8 \leqslant N, Z \leqslant 20$) are well described using the USD shell-model interaction developed by Brown and Wildenthal [1]. They show that the experimental g factors in this region are well reproduced using the free nucleon g factors. However, the properties of nuclei at the border of this region, with magic neutron number $N = 20$ and a mid-shell number of protons ($Z = 11, 12$), are found to deviate strongly from the predictions by the sd shell model. Nuclear masses and binding energies, excitation energies and β-decay properties, electromagnetic moments, all confirm that the ground states of the neutron rich Na and Mg isotopes with about twenty neutrons

* Corresponding author.
E-mail address: gerda.neyens@fys.kuleuven.be (G. Neyens).
[1] On leave from INRNE, Bulgarian Academy of Sciences, BG-1784 Sofia, Bulgaria.
[2] Present address: CNRS/IN2P3; Université Paris-Sud, UMR8609, CSNSM, ORSAY-Campus, F-91405, France.
[3] Present address: Centre d'Etudes Nucléaires de Bordeaux Gradignan—CENBG, UMR 5797 CNRS/IN2P3 Université Bordeaux 1, F-33175 Gradignan, France.

0370-2693/$ – see front matter
doi:10.1016/j.physletb.2006.10.026

Z = 14	Si	30	31	32	33	34	35	36
Z = 13	Al	29	30	31	32	33	34	35
Z = 12	Mg	28	29	30	31	32	33	34
Z = 11	Na	27	28	29	30	31	32	33
Z = 10	Ne	26	27	28	29	30	31	32
Z = 9	F	25	26	27		29		31
N =		16	17	18	19	20	21	22

Fig. 1. The island of inversion as defined initially from theory (box) and as established by now experimentally (nuclei in dark-grey). Nuclei in white are still under investigation, those in light-grey are in good agreement with the sd–pf shell model without considering excitations of neutrons across $N = 20$.

[2–7] are dominated by neutron excitations from the sd- into the pf-orbits (called 'intruder' states). The shell-model interaction has consequently been altered and the model space extended, in order to reproduce the unusual properties of these exotic nuclei. The earliest modification (Warburton et al., 1990 [8]) explains the special behavior of nuclei belonging to the so-called 'island of inversion', a region of nuclei with $Z = 10, 11, 12$ and $N = 20, 21, 22$. This name refers to the fact that the ground state wave function is dominated by particle-hole excitations of neutrons across the reduced $N = 20$ shell gap, which has experimentally been confirmed for the nuclei in dark-grey in Fig. 1. Later experiments have proven that also isotopes with $N = 18$ [6] or $N = 19$ [7] belong to this island of inversion. New interactions were developed (e.g. Caurier et al., 1998 [9]; Otsuka et al., 1999 [10]) as more experimental evidence became available. For the nuclei at the borders of this island, the different models predict different ground state properties, and thus experiments are needed to further refine the model parametrizations.

The Al isotopes with $Z = 13$ protons are located at the border of the island of inversion. Isotopes with just one proton more (Si) are known to have a normal shell structure at low energy [11,12], while the ground states of isotopes with one proton less (^{32}Mg ($N = 20$) and ^{31}Mg ($N = 19$)) are dominated by particle-hole (intruder) configurations [3,7,13]. Thus the transition from the 'normal' shell model region into the 'island of inversion' is expected to happen in the Al isotopes. Up to ^{31}Al ($N = 18$) the low-energy spectrum of these isotopes [14–16] is found to be in very good agreement with the USD shell-model. In ^{32}Al evidence for an intruder configuration around 1 MeV is found [17], while the ground state is suggested to be a normal sd-state based on a recent g factor measurement [14]. Also in ^{33}Al a low-lying state around 700 keV is suggested to be an intruder state [18], while no evidence for mixing with intruder configurations in the ground state is found from a β-decay study [19].

This Letter reports on the first precise measurements of the ground state g factors of the neutron rich Al isotopes from ^{31}Al up to ^{33}Al ($N = 20$). The obtained precision is a result of significant improvements in the experimental method and careful studies on the systematic errors. Such data can provide information on small admixtures of 2p–2h intruder configurations in the wave function of exotic nuclei, as demonstrated recently for the neutron-rich Na isotopes [20].

Neutron rich Al isotopes have been produced in the fragmentation of a $^{36}S^{16+}$ beam (77.5 MeV/u) on a ^{9}Be target ($\sim$1 mm). Secondary beams of ^{31,32,33}Al with purities of respectively 95–85–97% were selected using the high-resolution fragment separator LISE at GANIL [21,22]. A ^{9}Be wedge degrader of about 1 mm thickness (198 mg/cm^2) was used to obtain such high beam purities. Fragments were identified by standard energy loss versus time of flight measurements using Si pin diodes (500 μm thickness). Spin polarization was obtained by deflecting the primary beam by 2(1)° with respect to the spectrometer entrance where the fragmentation target was mounted. In order to obtain the highest polarization, fragments are selected in the wing of their longitudinal momentum distribution [23]. The polarized beam rates that were implanted in our crystal varied from 15000/s for ^{31}Al ($t_{1/2} = 644$ ms), 5000/s for ^{32}Al ($t_{1/2} = 33$ ms) to 1500/s for ^{33}Al ($t_{1/2} = 42$ ms [19]).

A detailed description of the experimental set-up and methodology can be found in [15,24]. A new movable crystal holder was installed in the vacuum chamber, on which several crystals can be mounted. This allowed easy identification of the best implantation host for maintaining the reaction induced polarization. Both metallic and ionic crystals have been investigated, all having a cubic lattice structure. A sufficiently high magnetic field is applied to maintain the spin orientation after implantation. The magnetic field is measured with a Hall probe at 7 cm from the crystal, the read-out being integrated in the data acquisition system. To calibrate the field at the position of the crystal a field mapping was performed before and after each experiment. The asymmetry in the β-decay of the polarized nuclei is observed in two scintillator telescopes. Scattering or noise events are excluded by requiring a coincidence between signals in a thin and a thick scintillator. The ratio of coincident counts in the Up and Down telescopes, $R = N_{\mathrm{up}}/N_{\mathrm{down}}$, is proportional to the amount of polarization in the implanted ensemble:

$$R = \left(\frac{N_{\mathrm{up}}}{N_{\mathrm{down}}}\right) = R_0\left(\frac{1 + A_1 B_1^0 Q_1^{\mathrm{exp}}}{1 - A_1 B_1^0 Q_1^{\mathrm{exp}}}\right) \approx R_0\left(1 + 2A_1 B_1^0 Q_1\right). \quad (1)$$

R_0 is the experimental asymmetry (e.g. due to different efficiency of both telescopes), A_1 is the asymmetry parameter of the β-decay, B_1^0 is the first order orientation tensor related to the spin-polarization and Q_1 quantifies the experimental asymmetry losses (e.g. due to relaxation, scattering of β-particles, experimental geometry, ...). A coil, which is part of a series LRC circuit, is placed around the implantation crystal to induce a radio-frequent (rf) field with frequency ν_{RF}. When this frequency matches the Larmor frequency $\nu_L = g\mu_N B_0/h$ the polarization in the ensemble is resonantly destroyed [25]. From this resonance frequency and the applied magnetic field, the g factor can be derived.

Before starting a g factor measurement, the experimental conditions to detect maximum polarization are optimized. All experiments have been done at room temperature. First the amount of polarization maintained in different crystals is investigated. Then the reaction-induced polarization is investigated as a function of the longitudinal momentum of the selected frag-

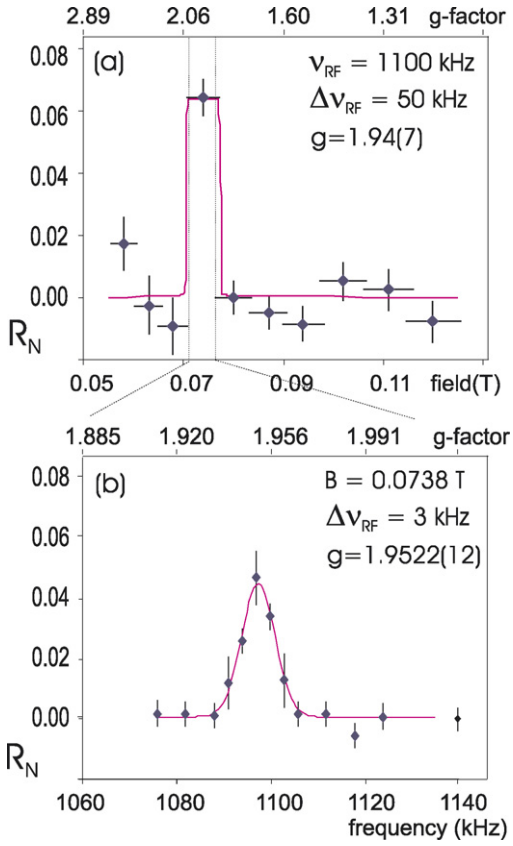

Fig. 2. NMR scans for ^{32}Al in Si as a function of the field (a) and as a function of the rf-frequency (b).

ment beam. The procedure for this is described in [26]. The polarization of the Al isotopes is maintained best in a Si single crystal (asymmetries up to 6% were observed) while this was up to 2 and 3 times less in MgO and NaCl.

Once polarization is established, it can be resonantly destroyed by the rf-field. Each rf-frequency was modulated continuously around a fixed value over a modulation range: $\nu_{RF} \pm \Delta\nu_{RF}$. When the applied frequency range covers the Larmor frequency, the polarization is destroyed and this is reflected as a change in the β-decay asymmetry. The resonance condition can be searched by changing the magnetic field B_0 or the rf-frequency. The normalized asymmetry R_N is plotted, such that one can directly deduce the amount of polarization destroyed at resonance:

$$R_N = \frac{R - R_{\text{base}}}{R} \approx -2A_1\sqrt{\frac{3I}{I+1}}\,P\,Q_1^{\text{exp}}. \tag{2}$$

The baseline R_{base} of the resonance curves is defined by measuring the β-decay asymmetry without rf-field applied.

Since a series LRC circuit with a narrow power peak (FWHM $\sim$ 100 kHz) is used to generate a high-power rf-signal, only a small g factor range can be scanned as a function of frequency (Fig. 2(b)). For isotopes with unknown ground state structure, we first search in a large g factor range by changing the static magnetic field B_0. The rf-frequency is fixed to a certain value and modulated over a broad range. Like that an extended g factor region can be scanned with a few values of B_0, as demonstrated in Fig. 2(a). All data were taken in a sweep mode in order to average out experimental asymmetry fluctuations during the measurement. The static field is changed every two minutes and during the field change (about 3 s) no data are collected. For every field value data are collected with and without rf-field to determine R_{base}. The rf-frequency is modified every ten seconds in a frequency scan because the rf-frequency changes instantaneously. R_{base} is determined after each full sweep in this case.

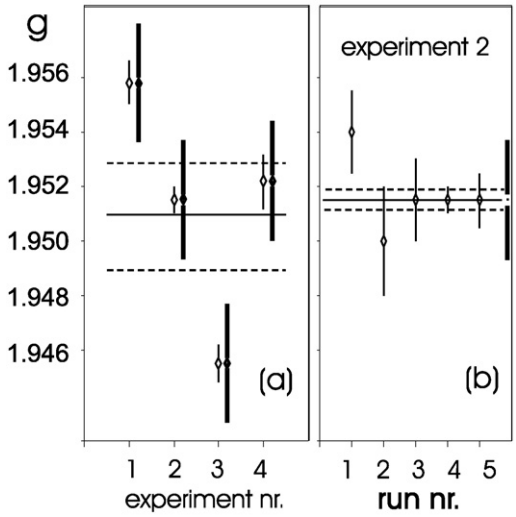

Fig. 3. (a) The most precise g factor results for ^{32}Al obtained in different experiments (with their statistical and total error). The dashed line illustrates the uncertainty in the field calibration. (b) Results obtained from different measurements during experiment 2. The total error on the weighted mean (shown on the right) includes the systematic error.

The observed NMR data are fit with a theoretical curve that is obtained by numerically solving the time evolution equation with a Hamiltonian that describes the time-dependent interaction of the nuclei with the static magnetic field and the modulated rf-field. An inhomogeneous line broadening of the NMR resonance is taken into account by convoluting the resulting resonance with a Gaussian line shape. More details are given in [26]. The statistical error on the g factor is deduced by fitting the data with the calculated function, using a multi-parameter χ^2-minimization procedure with the g factor (determining the resonance position) and the amount of destroyed polarization (determining the amplitude) as parameters. The rf-field strength and the Gaussian line width (determining the line shape and width) are determined by making a consistent fit of many resonance curves taken for different rf-conditions [26]. This was done for the Al isotope with the highest NMR amplitude, namely ^{32}Al. The systematic uncertainty on our data is investigated by measuring NMR resonances for ^{32}Al in Si during four different experiments. The error due to the magnetic field calibration, which is made for every experiment independently, is derived from the scattering on these values. The standard deviation is 0.11% as shown in Fig. 3(a), and this will be taken as our systematic error. This systematic error is almost an order of magnitude larger than most statistical errors. As final error the square root of the sum of the squared statistical and system-

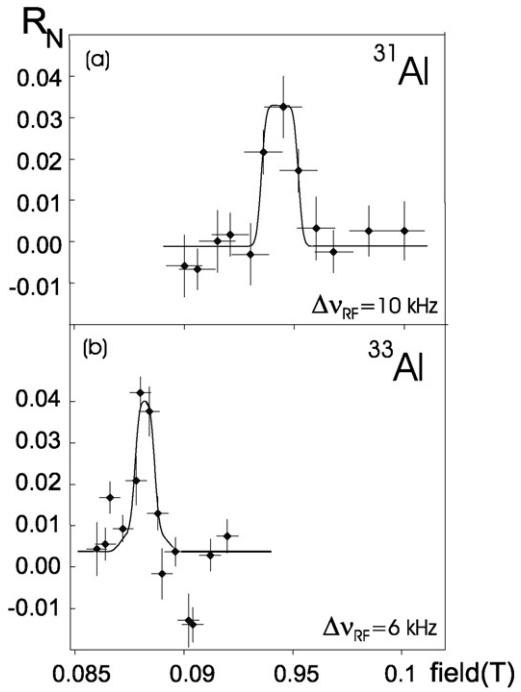

Fig. 4. NMR scans as a function of the magnetic field for ^{31}Al (a) and ^{33}Al (b) implanted in a Si single crystal. The applied frequency is 1100 kHz.

atic uncertainties is used. This total error is shown as well on the data points of Fig. 3(a), demonstrating that with this error a normal statistical ensemble is obtained. In Fig. 3(b) the results of five measurements on ^{32}Al, obtained during the same experiment, are presented. The weighted mean value of these five measurements gives $g = 1.9516(4)$, and including the systematic error we obtain $g(^{32}\mathrm{Al}) = 1.9516(22)$. This value is in agreement with the earlier reported value $g = 1.959(9)$ [14].

As the g factor of ^{31}Al was known from [15], a field scan with a small frequency modulation $\nu_{\mathrm{RF}} = (1100 \pm 10)$ kHz was performed (Fig. 4(a)). The deduced value $g(^{31}\mathrm{Al}) = 1.532(2)$, which includes also a 0.11% systematic error, is in a good agreement with the earlier published value $g = 1.517(20)$ [15]. The measurement on ^{33}Al was performed during the same experiment: First a field scan was measured with the same rf-frequency and a large modulation $\nu_{\mathrm{rf}} = (1100 \pm 50)$ kHz from which we deduced $g = 1.68(6)$. Then a fine scan is made (Fig. 4(b)), resulting in $g(^{33}\mathrm{Al}) = 1.635(2)$.

The experimental g factors and level schemes of $^{30\text{–}33}$Al are compared to the results from large scale shell model calculations performed with the Antoine code [27]. Two interactions have been used: The USD interaction [1] with protons and neutrons restricted to the sd-shell and the sdpf–sm interaction [4] with different model spaces for the neutrons. All g factors are calculated using free nucleon values for g_s and g_l. The experimental level schemes and g factors of ^{30}Al and ^{31}Al (Fig. 5) are in very good agreement with the calculated ones. A less good agreement is observed for ^{32}Al: The first two excited states observed by Robinson et al. [28] are inverted with respect to the calculations, and the suggested 1p–1h intruder state observed by Fornal et al. [17] is reproduced only by the sdpf–sm calculation if the neutron model space includes the $f_{7/2}p_{3/2}$ orbits. Thus the first three excited states in ^{32}Al do not support a normal sd shell-model picture. In Table 1 the g factors of all odd–even and odd–odd Al isotopes are compared to the calculated values and a good general agreement is observed (less than 2% deviation for most isotopes). For ^{32}Al the 6% higher experimental value cannot be attributed to a missing intruder contribution in the ground state wave function. Such a 2p–2h contribution would significantly lower the g factor, as a pure 2p–2h configuration has $g(^{32}\mathrm{Al}, \text{2p–2h}, 1^+) = 0.34$. Thus the deviation is entirely due to the composition of the wave function in the sd-shell.

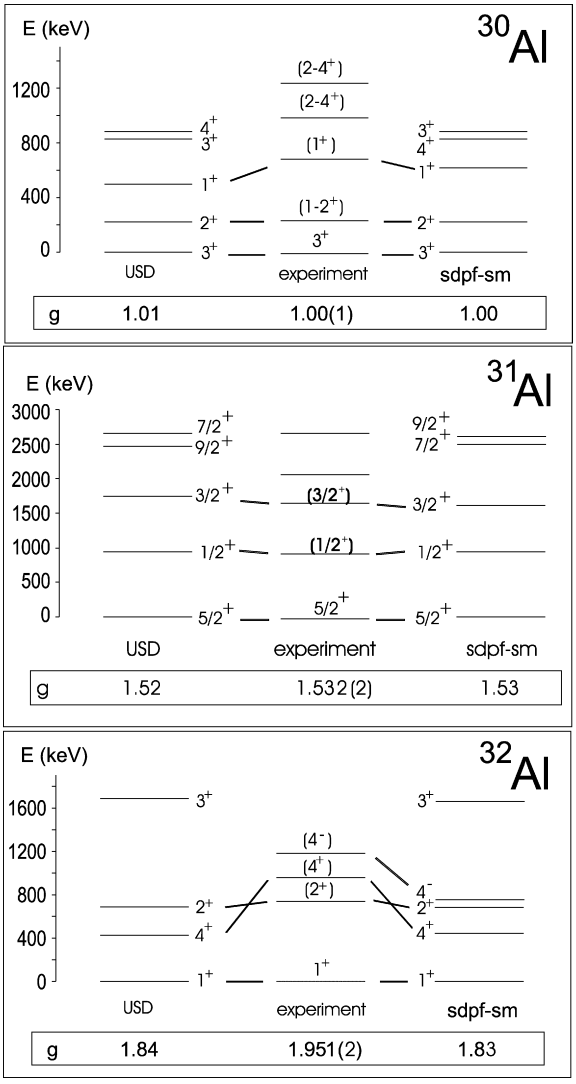

Fig. 5. Comparison between calculated and experimental level schemes and g factors for ^{30,31,32}Al.

In trying to understand the possible origin of this deviation, we performed calculations in different restricted model spaces for the protons (Fig. 6). The major contribution in the ^{32}Al wave function comes from the $(\pi d_{5/2}\nu d_{3/2})_{1^+}$ configuration, for which the Schmidt value is $g(\pi d_{5/2}\nu d_{3/2}, 1^+) = 2.78$ using the additivity rule [29]. All other sd-shell configurations have a Schmidt value below 1, thus lowering the calculated g factor with respect to this Schmidt value as illustrated in Fig. 6. No-

Table 1
Experimental and theoretical g factors of Al isotopes (calculated with neutrons in the sd-shell). The deviation between experimental and calculated values is given in brackets. (∗) are data from this work, the others are taken from [14] and [30]

A	N	Spin	Lifetime	g_{exp}	g_{USD}	$g_{\text{sdpf–sm}}$
Odd–even						
33	20	5/2+	44 ms	1.635(2)*	1.702 (3.9%)	1.702 (3.9%)
31	18	5/2+	640 ms	1.532(2)*	1.525 (−0.5%)	1.524 (−0.5%)
29	16	5/2+	6.56 min		1.485	1.483
27	14	5/2+	stable	1.4566	1.435 (−1.5%)	1.428 (−2.0%)
25	12	5/2+	7.183 s	1.4582(5)	1.485 (1.8%)	1.488 (2.0%)
Odd–odd						
32	19	1+	33 ms	1.9516(22)*	1.843 (−5.9%)	1.834 (−6.4%)
30	17	3+	3.60 s	1.003(2)	1.011 (0.8%)	1.000 (−0.3%)
28	15	3+	2.24 min	1.081(2)	1.026 (−5.2%)	1.027 (−5.3%)
26	13	5+	stable	0.560(1)	0.567 (1.2%)	0.567 (1.2%)

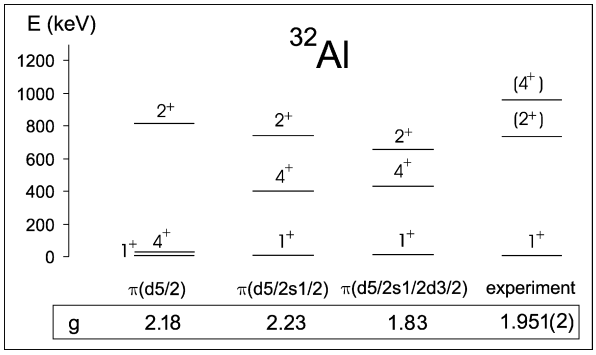

Fig. 6. Calculation with the sdpf-sm interaction for different restrictions in the proton model space and neutrons in sd-shell only.

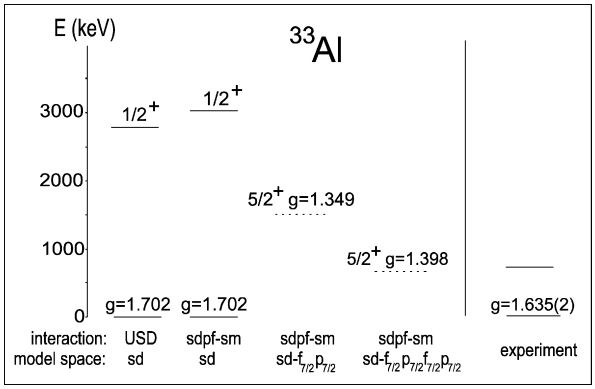

Fig. 7. Calculations for $0p$–$0h$ states (in the sd-shell) and for 2p–2h states in a reduced or full sdpf space.

tice that the ground state g factor and the energies of the excited states are sensitive to different components in the wave function: The g factor is hardly modified by including the $\pi s_{1/2}$ orbit while the energy of the 4^+ state is modified drastically. On the other hand, by including also the $\pi d_{3/2}$ orbital the level scheme remains similar, while it strongly reduces the g factor. This illustrates that g factors and excitation energies should both be considered when fitting the parameters for a new interaction. Less contribution from the $\pi d_{3/2}$ orbit would lead to a better agreement for both the g factor and the energies of the first excited states in ^{32}Al. This suggests that the $Z = 16$ shell gap might play a role in explaining the disagreement for both the ^{32}Al g factor and its energy level scheme.

For the odd Al isotopes the experimental g factors all deviate less than 2% from the calculated values (Table 1), except for the semi-magic ^{33}Al ($N = 20$) which deviates almost 4%. Furthermore, one expects the lowest excited state around 3 MeV (a nearly pure $\pi s_{1/2}$ state) if no excitations of neutrons are allowed across the $N = 20$ shell gap (Fig. 7). Experimentally, the first excited state is observed as low as 730 keV [18], and it was suggested that this is a 2p–2h $5/2^+$ intruder state. With the sdpf–sm interaction a pure 2p–2h intruder state appears indeed around 1.5 MeV in a reduced $f_{7/2}p_{3/2}$ space and around 650 keV if the full pf space is used (right part of Fig. 7). The g factor of these intruder states is lower than that of the sd shell state, and the experimental value is found to be in-between both. Thus a configuration where some amount of intruder configurations is mixed with the normal sd shell configuration could explain the observed ground state g factor. With the present sdpf–sm interaction, the calculated g factor reduces (from $1.702 \rightarrow 1.689 \rightarrow 1.680$) if two neutrons are allowed in the reduced or full pf space, due to the fact that a small amount of intruder components occurs (up to 10% in these calculations). This suggests that intruder configurations do play an important role in the low-energy structure of ^{33}Al and that in the present interaction this amount is too low. Note that the half-life and branching ratio for both β and β-delayed neutron decay of ^{33}Al has been well-described by the sd shell-model [19], illustrating again that different observables are sensitive to different parts of the wave function.

Our experimental value suggests that the amount of intruder mixing is at least 25%. This is supported by calculations performed by Utsuno et al. using the Monte Carlo Shell Model in the sd–$p_{3/2}f_{7/2}$ model space with the SDPF-M interaction [10]. They predict that the ground state of ^{33}Al has 50% of intruder mixture with a g factor $g(^{33}\text{Al})_{\text{MCSM}} = 1.55$ [31] (using free nucleon values). Later, the interaction was modified in its monopole part as to reproduce the experimental g factors and quadrupole moments of the Na isotopes (Fig. 8) and using effective g factors [20]. The value for ^{33}Al calculated with this modified interaction and effective g factors [32] is in very good agreement with our experimental number, as shown on (Fig. 8).

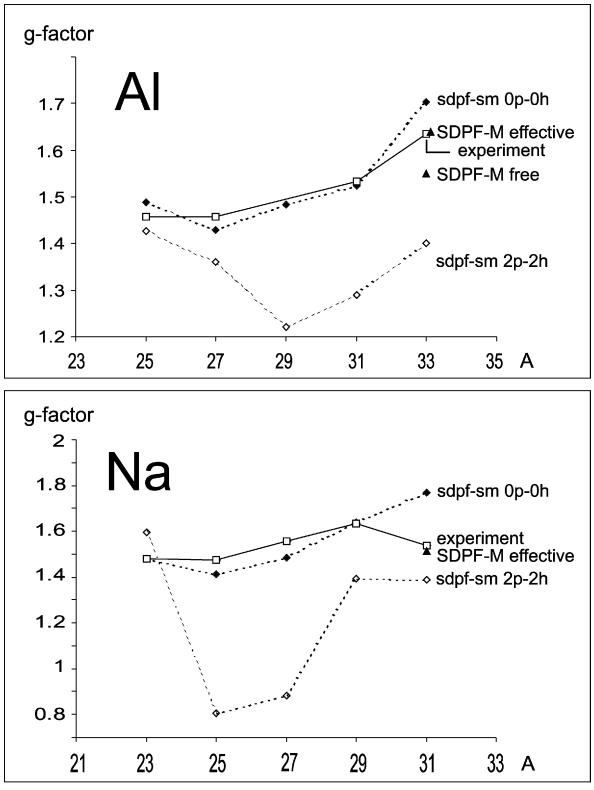

Fig. 8. Experimental g factors of odd Na isotopes and Al isotopes compared to predictions with the sdpf–sm interaction for 0p–0h and 2p–2h configurations, and with the SDPF-M interaction (see text).

In conclusion, the g factors of exotic Al-isotopes, produced via projectile-fragmentation reactions, were measured with the NMR technique, after optimizing all NMR conditions. This has lead to a significant amount of polarization (up to 3.5%), allowing precision studies for the g factors up to the $N = 20$ nucleus ^{33}Al. The results are compared with large scale shell model calculations. The nuclear properties of ^{30}Al and ^{31}Al are in very good agreement with the theoretical predictions in the sd-shell model space, placing these isotopes clearly outside the island of inversion. No evidence for the presence of intruder configurations in the ground state of ^{32}Al was found, but the experimental level scheme and the ground state g factor might be better reproduced with an enhanced $Z = 16$ shell gap. For ^{33}Al, the first indication is observed for a non-negligible (at least 25%) contribution of intruder configurations into the ground state wave function. The sdpf–sm interaction does not predict enough intruder mixing in order to explain the measured g factor.

Acknowledgements

This work has been supported by the European Community FP6—Structuring the ERA—Integrated Infrastructure Initiative contract EURONS No. RII3-CT-2004-506065. P.H. is grateful to the IWT-Vlaanderen (Institute for the Promotion of Innovation through Science and Technology in Flanders) for providing a scholarship. This work was supported also by INTAS 00-463, the IUAP project No. p5-07 of OSCT Belgium and by the FWO-Vlaanderen. D.L.B. acknowledges support through grant BgNSF VUF06/05.

References

[1] B.A. Brown, B.H. Wildenthal, Annu. Rev. Nucl. Part. Sci. 38 (1988) 29.
[2] C. Thibault, et al., Phys. Rev. C 12 (1975) 644.
[3] T. Motobayashi, et al., Phys. Lett. B 346 (1995) 9.
[4] S. Nummela, et al., Phys. Rev. C 63 (2001) 044316.
[5] S. Nummela, et al., Phys. Rev. C 64 (2001) 054313.
[6] M. Keim, et al., Eur. Phys. J. A 8 (2000) 31;
M. Keim, et al., AIP Conf. Proc. 455 (1998) 50.
[7] G. Neyens, et al., Phys. Rev. Lett. 94 (2005) 022501.
[8] E.K. Warburton, J.A. Becker, B.A. Brown, Phys. Rev. C 41 (1990) 1147.
[9] E. Caurier, et al., Phys. Rev. C 58 (1998) 2033.
[10] Y. Utsuno, et al., Phys. Rev. C 60 (1999) 054315.
[11] P.M. Endt, et al., Nucl. Phys. A 521 (1990) 1.
[12] N. Iwasa, et al., Phys. Rev. C 67 (6) (2003) 064315.
[13] O. Niedermaier, et al., Phys. Rev. Lett. 94 (2005) 172501.
[14] H. Ueno, et al., Phys. Lett. B 615 (2005) 186.
[15] D. Borremans, et al., Phys. Lett. B 537 (2002) 45.
[16] F. Marechal, et al., Phys. Rev. C 72 (2005) 044314.
[17] B. Fornal, et al., Phys. Rev. C 55 (1997) 2.
[18] W. Mittig, et al., Eur. Phys. J. A 15 (2002) 157.
[19] A.C. Morton, et al., Phys. Lett. B 544 (2002) 274.
[20] Y. Utsuno, et al., Phys. Rev. C 70 (2004) 044307.
[21] R. Anne, et al., Nucl. Instrum. Methods A 257 (1987) 215.
[22] R. Anne, et al., Nucl. Instrum. Methods B 70 (1992) 276.
[23] D. Borremans, et al., Phys. Rev. C 66 (2002) 054601.
[24] K. Turzo, et al., Phys. Rev. C 73 (2006) 044313.
[25] N. Coulier, et al., Phys. Rev. C 59 (1999) 1935.
[26] P. Himpe, et al., Ph.D. Thesis, K.U. Leuven, 2006 (unpublished).
[27] E. Caurier, F. Nowacki, Acta Phys. Pol. 30 (1999) 705.
[28] M. Robinson, et al., Phys. Rev. C 53 (1996) R1465.
[29] G. Neyens, Rep. Prog. Phys. 66 (2003) 633;
G. Neyens, Rep. Prog. Phys. 66 (2003) 1251, Erratum.
[30] N.J. Stone, At. Data Nucl. Data Tables 90 (2005) 75.
[31] Y. Utsuno, et al., Phys. Rev. C 64 (2001) 0011301(R).
[32] T. Otsuka, private communication.